Electronic Supplementary Material (ESI) for Journal of Materials Chemistry C.
This journal is © The Royal Society of Chemistry 2024

Supporting Information

$Ca_{18}Na_3Y(PO_4)_{14}:Eu^{2+},Mn^{2+}$: A Novel Single-Phase Dual-Emission Phosphor and Its Spectral Modulation by Mg^{2+} for Plant Lighting and WLEDs

Zhibin Ye [a], Ziwang Zhang [b], Nan Yang [a], Zhuo Li [a], Weijie Huang [a] and Jianxin Shi*[,a]

[a] *School of Chemistry, IGCME, Sun Yat-Sen University, Guangzhou 510006, P. R. China.*

[b] *School of Materials, Sun Yat-Sen University, Shenzhen 518107, P. R. China.*

* Corresponding author: cessjx@mail.sysu.edu.cn.

Table of contents

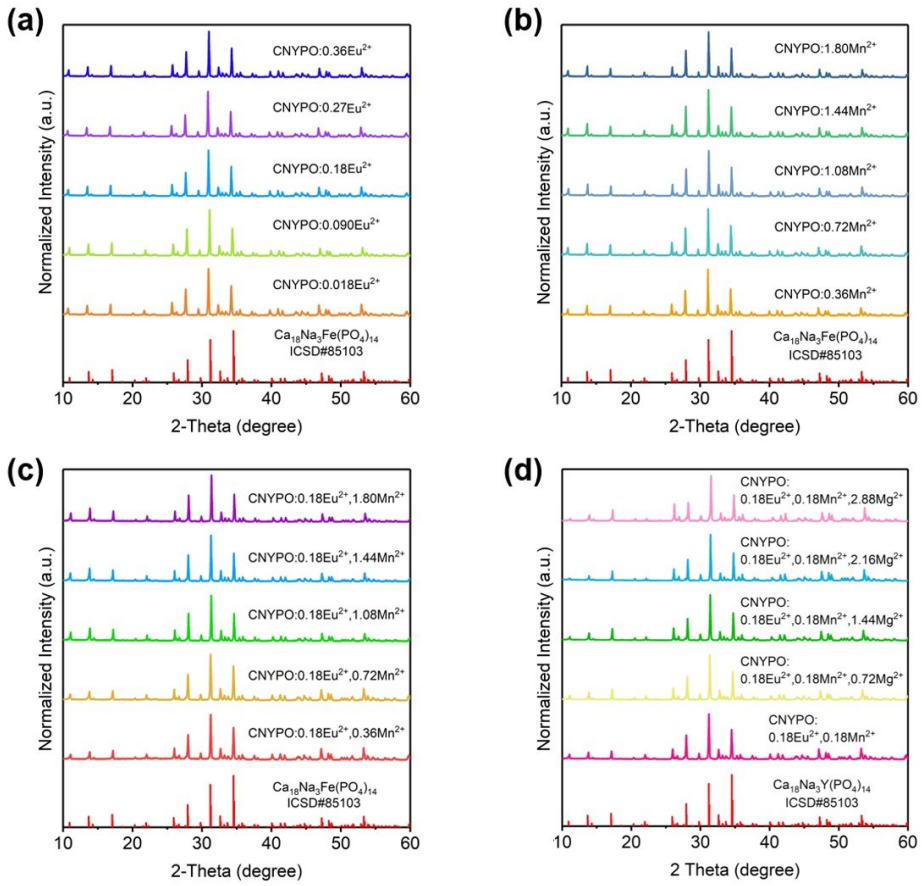

Fig. S1 The XRD patterns of (a) CNYPO:xEu^{2+}, (b) CNYPO:yMn^{2+}, (c) CNYPO:0.18Eu^{2+},yMn^{2+}, and (d) CNYPO:0.18Eu^{2+},0.18Mn^{2+},zMg^{2+}.

It is clear from all the XRD patterns that there are no additional reflections, indicating that the introduction of dopant ions does not produce impurity phase.

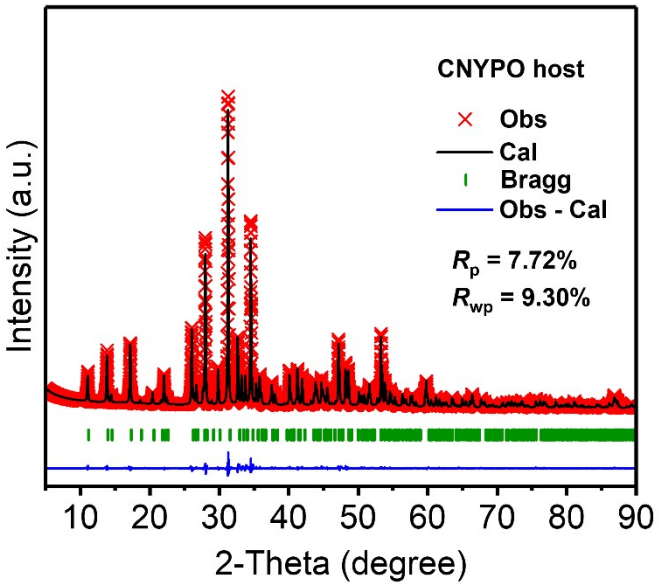

Fig. S2 The XRD pattern and Rietveld refinement of CNYPO host.

Table S1. The crystallographic parameters, atomic coordinates and site occupancies of CNYPO host.

Space group			$R3c$ (No.161)			
Cell parameters			$a = b = 10.4499$ Å, $c = 37.3199$ Å $\alpha = \beta = 90°$, $\gamma = 120°$ $V = 3529.3351$ Å^3, $Z = 3$			
Reliability factors			$R_p = 7.72\%$, $R_{wp} = 9.30\%$			
Atom	Site	Occup.	x	y	z	U_{iso} (Å^2)
Ca1	18*b*	1	0.72871	0.85455	0.43422	0.0187
Ca2	18*b*	1	0.62025	0.82529	0.23435	0.0224
Ca3	18*b*	0.833	0.12307	0.26564	0.32733	0.0242
Na1	18*b*	0.167	0.12307	0.26564	0.32733	0.0242
Na2	6*a*	1	0	0	0.18015	0.0795
Ca4	6*a*	0.5	0	0	0.00726	0.0324
Y1	6*a*	0.5	0	0	0.00726	0.0324
P1	6*a*	1	0	0	0.27164	0.0431
P2	18*b*	1	0.69433	0.87699	0.13771	0.0315
P3	18*b*	1	0.64805	0.83769	0.03825	0.0289
O1	6*a*	1	0	0	0.30055	0.0127
O2	18*b*	1	0.01008	0.86421	0.25445	0.0376
O3	18*b*	1	0.73615	0.90838	0.17248	0.0317
O4	18*b*	1	0.75465	0.75279	0.12316	0.0436
O5	18*b*	1	0.74089	0.01686	0.11379	0.0318
O6	18*b*	1	0.5052	0.78947	0.11982	0.0265
O7	18*b*	1	0.60293	0.96018	0.04587	0.0267
O8	18*b*	1	0.56893	0.67537	0.04982	0.0144
O9	18*b*	1	0.81524	0.90548	0.04386	0.0162
O10	18*b*	1	0.64601	0.85494	0.99004	0.0268

Table S2. The crystallographic parameters, atomic coordinates and site occupancies of CNYPO:0.18Eu^{2+},0.18Mn^{2+}.

Space group			*R*3*c* (No.161)			
Cell parameters			$a = b = 10.4452$ Å, $c = 37.3279$ Å $\alpha = \beta = 90°$, $\gamma = 120°$ $V = 3527.3351$ Å^3, $Z = 3$			
Reliability factors			$R_p = 8.54\%$, $R_{wp} = 6.09\%$			
Atom	Site	Occup.	*x*	*y*	*z*	U_{iso} (Å^2)
Ca1	18*b*	1	0.72486	0.85217	0.43396	0.0083
Ca2	18*b*	1	0.61892	0.81956	0.23405	0.0064
Ca3	18*b*	0.833	0.12457	0.26769	0.32839	0.0071
Na1	18*b*	0.167	0.12457	0.26769	0.32839	0.0071
Na2	6*a*	1	0	0	0.18134	0.0836
Ca4	6*a*	0.5	0	0	0.00231	0.0224
Y1	6*a*	0.5	0	0	0.00231	0.0224
P1	6*a*	1	0	0	0.26829	0.0195
P2	18*b*	1	0.6892	0.87271	0.1362	0.0110
P3	18*b*	1	0.65118	0.83333	0.03449	0.0214
O1	6*a*	1	0	0	0.30547	0.0082
O2	18*b*	1	0.01347	0.86686	0.24778	0.0294
O3	18*b*	1	0.7427	0.8977	0.17342	0.0272
O4	18*b*	1	0.76233	0.76042	0.12376	0.0231
O5	18*b*	1	0.74061	0.01704	0.1133	0.0244
O6	18*b*	1	0.50868	0.76687	0.12427	0.0219
O7	18*b*	1	0.59962	0.95756	0.04648	0.0208
O8	18*b*	1	0.56996	0.67882	0.04704	0.0120
O9	18*b*	1	0.81891	0.92155	0.04189	0.0124
O10	18*b*	1	0.63881	0.83816	0.98915	0.0185

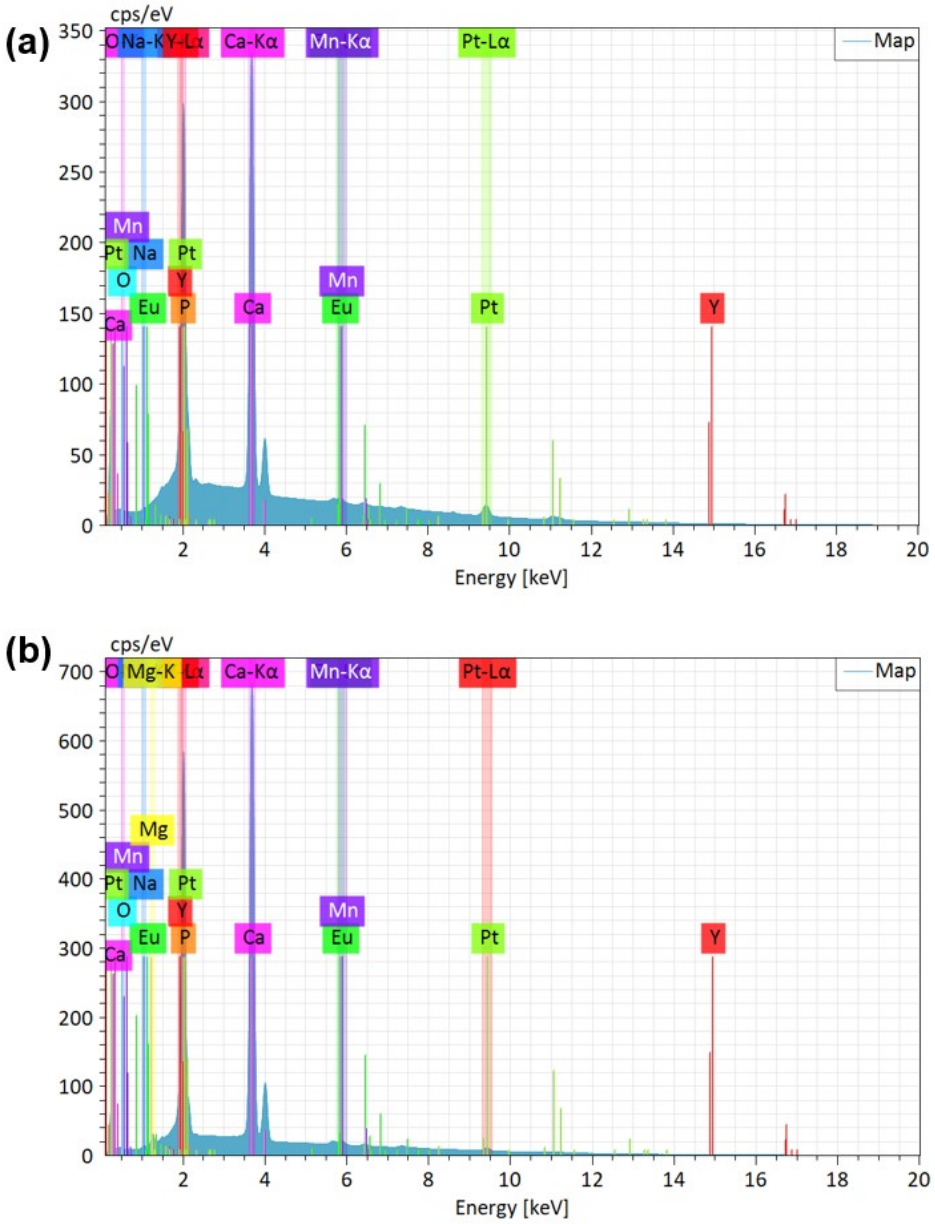

Fig. S3 The EDS of (a) CNYPO:0.18Eu^{2+},0.18Mn^{2+} and (b) CNYPO:0.18Eu^{2+},0.18Mn^{2+},2.88Mg^{2+}.

Fig. S3 depicts the EDS of CNYPO:0.18Eu^{2+},0.18Mn^{2+} and CNYPO:0.18Eu^{2+}, 0.18Mn^{2+},2.88Mg^{2+}. It is clear that Eu^{2+}, Mn^{2+} and Mg^{2+} have been doped into the CNYPO host successfully. Pt is detected in the result due to the fact that Pt is used as a conductive coating introduced by low vacuum sputter coating so that the contrast can be improved.

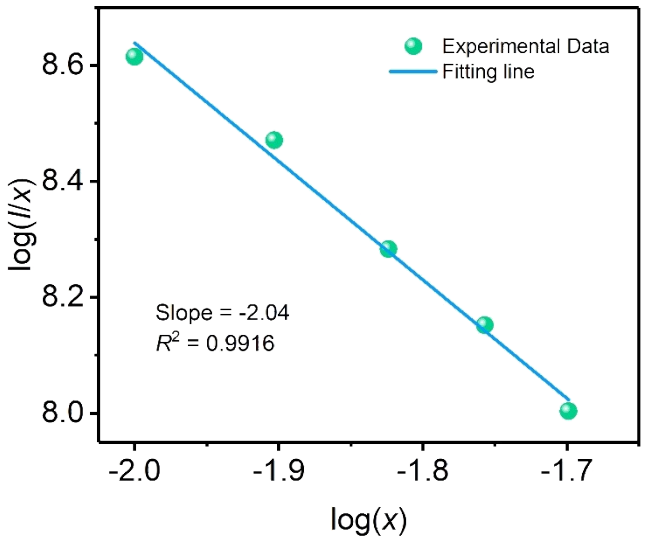

Fig. S4 The relationship between log(*I*/*x*) and log(*x*) of CNYPO:*x*Eu^{2+}

The concentration quenching is usually dominated by exchange interaction or electric multipolar interaction.[1] The interaction in CNYPO:*x*Eu^{2+} may be determined by the critical distance (R_C) of Eu^{2+} in CNYPO host, given by the equation:[2]

$$R_C = 2\left(\frac{3V}{4\pi x_C N}\right)^{\frac{1}{3}} \quad (1)$$

where V is the volume of the unit cell, x_C is the concentration of Eu^{2+} when the concentration quenching occurs, and N is the number of Ca^{2+} ions in the unit cell. For CNYPO:0.18Eu^{2+}, V = 3529.3351 Å^3, x_C = 0.01, N = 54. As a result, R_C is calculated to be 22.64 Å, which is larger than 5 Å. Hence, the concentration quenching effect of Eu^{2+} in CNYPO host is attributable to electric multipolar interaction. The type of electric multipolar interaction can be fitted by the Dexter equation:[3]

$$\log\left(\frac{I}{x}\right) = \log k - \frac{S}{d}\log(x) \quad (2)$$

where I is the emission intensity, d is the dimension of energy transfer equaling to 3, and S is the index of electric multipolar. S = 6, 8 and 10 corresponds to dipole-dipole, dipole-quadrupole and quadrupole-quadrupole interaction, respectively. The integrated emission intensities of CNYPO:*x*Eu^{2+} ($x \geq x_C$) have been used for fitting, and the results are shown in Fig. S4. Since the slope of the fitting line is –2.04, the S equals to 6.12, the

concentration quenching effect of CNYPO:xEu^{2+} is dominated by dipole-dipole interaction.

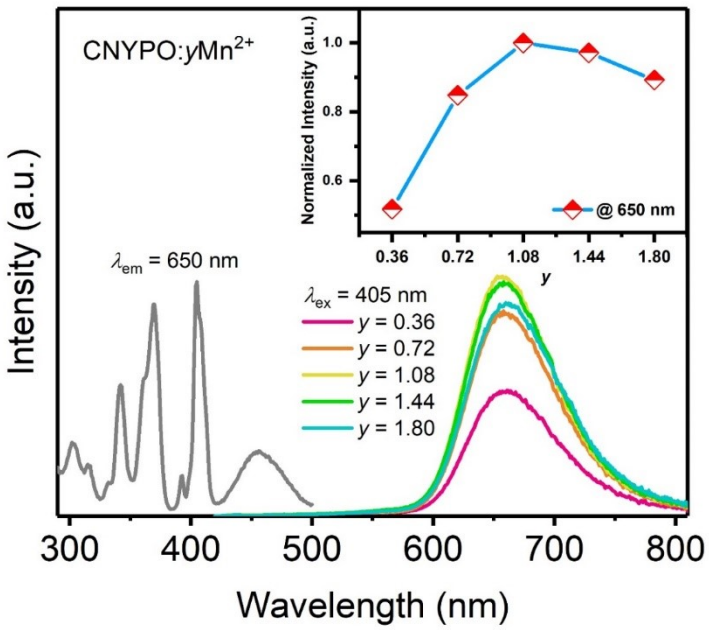

Fig. S5 PLE and PL spectra of CNYPO:yMn^{2+} (the inset shows the emission intensity at 650 nm for variable concentration of Mn^{2+}).

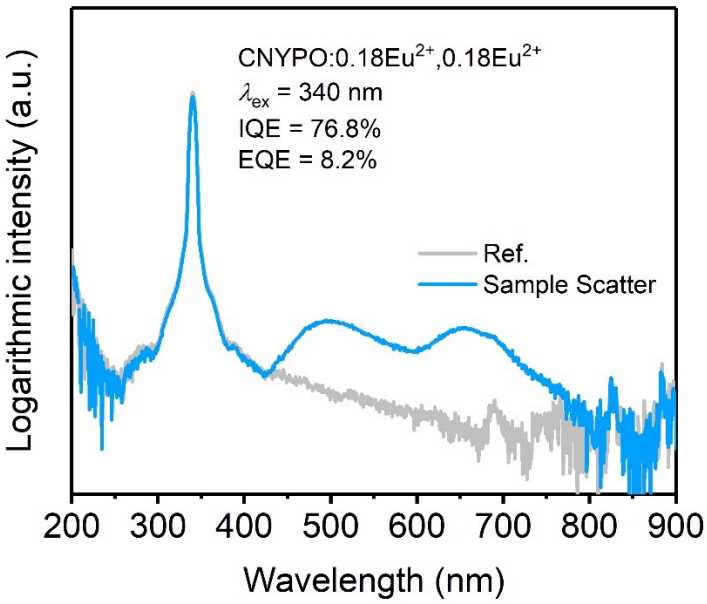

Fig. S6 IQE of CNYPO:0.18Eu^{2+},0.18Mn^{2+} under the excitation of 340 nm.

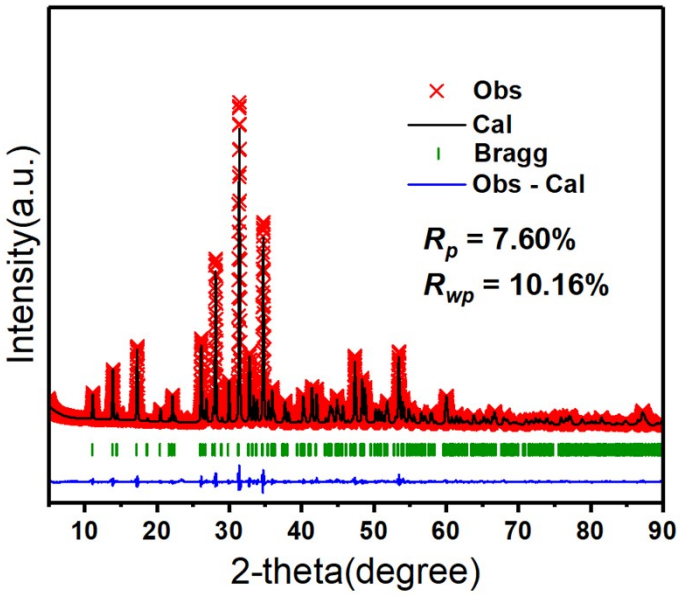

Fig. S7 The XRD pattern and Rietveld refinement of CNYPO:0.18Eu^{2+},0.72Mn^{2+}.

Table S3. The refined cell parameters of CNYPO:0.18Eu^{2+},0.72Mn^{2+}.

	Reliability factors	Cell parameters
CNYPO:0.18Eu^{2+},0.72Mn^{2+}	R_p = 7.60% R_{wp} = 10.16%	$a = b$ = 10.4251 Å, c = 37.2506 Å $\alpha = \beta$ = 90°, γ = 120° V = 3506.0730 Å^3, Z = 3

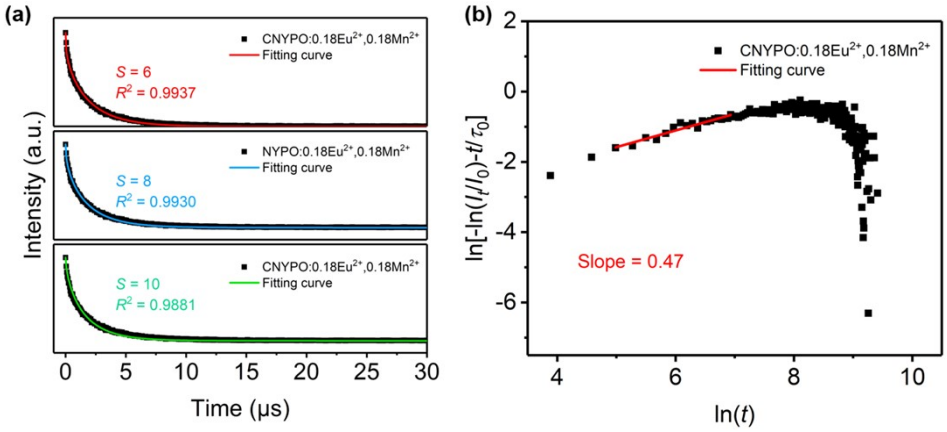

Fig. S8 (a) The Inokuti-Hirayama fitting curves and (d) the linear fitting curve of $\ln[-\ln(I_t/I_0)-t/\tau_0]$ to $\ln(t)$ of CNYPO:0.18Eu^{2+},0.18Mn^{2+}.

The Inokuti-Hirayama modal has been used to fit the decay curve of CNYPO:0.18Eu^{2+},0.18Mn^{2+}: [4, 5]

$$I_t = I_0 \exp\left[-\frac{t}{\tau_0} - Q\cdot t^{\frac{3}{S}}\right] \#(3)$$

$$\ln\left[-\ln\frac{I_t}{I_0} - \frac{t}{\tau_0}\right] = A + \frac{3}{S}\ln(t) \#(4)$$

where I_0 and I_t represent the luminescent intensity at t = 0 and t, respectively, τ_0 is the lifetime of donors without acceptors (2.590 μs as shown in Fig. 4b), Q stands for the macroscopic parameter, and S is the index of electric multipolar. S = 6, 8 and 10 corresponds to dipole-dipole, dipole-quadrupole and quadrupole-quadrupole interaction, respectively. The fitting results of each value of S are presented in Fig. S8a, the curve fitting is optimal when S = 6, indicating that dipole-dipole interaction should be the dominant energy transfer mechanism in CNYPO:Eu^{2+},Mn^{2+}. As shown in Fig. S8b, the slope of the fitting line equals to 0.47, therefore, S = 3/0.47 = 6.38, which is close to 6. The result is consist with that of Eq. 3.

Table S4. The bond length of the Ca sites occupied by Eu^{2+} in CNYPO:0.18Eu^{2+},0.18Mn^{2+} and CNYPO:0.18Eu^{2+},0.18Mn^{2+},2.88Mg^{2+} calculated by XRD refinement results.

Formula	CNYPO: 0.18Eu^{2+},0.18Mn^{2+}	CNYPO: 0.18Eu^{2+},0.18Mn^{2+},2.88Mg^{2+}
Reliability factors	R_p = 8.54%, R_{wp} = 6.09%	R_p = 8.87%, R_{wp} = 12.45%
Bond	Bond length (Å)	Bond length (Å)
Ca1-O2	2.52	2.45
Ca1-O5	2.62	2.51
Ca1-O6	2.29	2.33
Ca1-O6	2.41	2.52
Ca1-O7	2.38	2.59
Ca1-O8	2.37	2.37
Ca1-O10	2.24	2.27
Ca2-O2	2.30	2.10
Ca2-O3	2.53	2.67
Ca2-O4	2.39	2.42
Ca2-O5	2.24	2.20
Ca2-O7	2.69	2.64
Ca2-O8	2.77	2.41
Ca2-O9	2.43	2.38
Ca2-O9	2.50	2.46
Ca3-O1	2.56	2.79
Ca3-O3	2.48	2.73
Ca3-O4	2.36	2.50
Ca3-O5	2.42	2.47
Ca3-O7	2.36	2.14
Ca3-O8	2.44	2.33
Ca3-O10	2.68	2.63
Ca3-O10	2.57	2.63

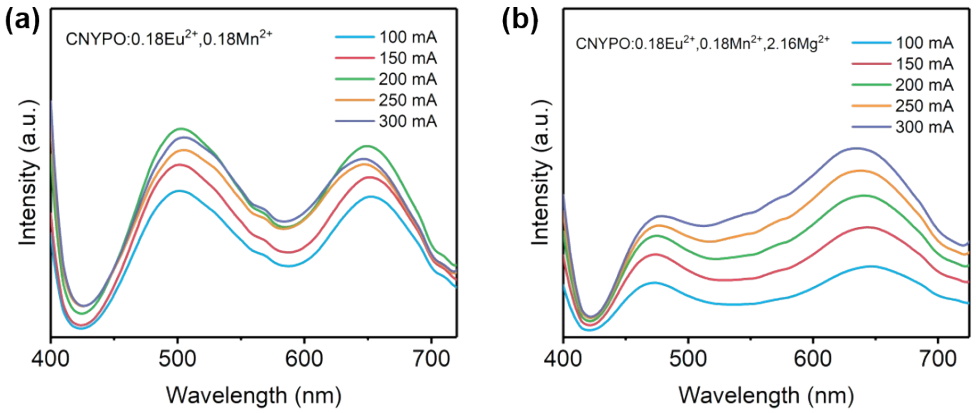

Fig. S9 Current-dependent EL spectra of the LED devices fabricated by (a) CNYPO:0.18Eu^{2+},0.18Mn^{2+} and (b) CNYPO:0.18Eu^{2+},0.18Mn^{2+},2.16Mg^{2+} with 365 nm chips, respectively.

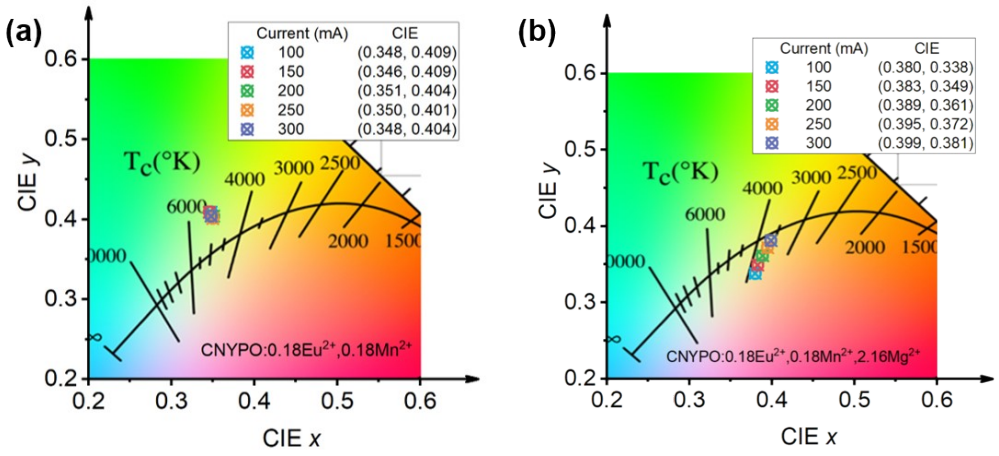

Fig. S10 CIE coordinates of the LED devices fabricated by (a) CNYPO:0.18Eu^{2+},0.18Mn^{2+} and (b) CNYPO:0.18Eu^{2+},0.18Mn^{2+},2.16Mg^{2+} with 365 nm chips, respectively.

The EL spectra and CIE coordinates of as-prepared devices are shown in Fig. S9 and S10, respectively. It can be seen that the shape and peak position of the EL spectra have little variation for the device fabricated by CNYPO:0.18Eu^{2+},0.18Mn^{2+}, and the CIE coordinates of that indicate a stable emission colour under various currents. For the device fabricated by CNYPO:0.18Eu^{2+},0.18Mn^{2+},2.16Mg^{2+}, the emission intensity of red component enhances as the current increases, and the CIE coordinates of the device shift slightly within the warm white light region. In general, the shape of spectra and emission color of the devices are stable under different currents.

References

1 X. Zhang, J. Su, X. Yan, Y. Liao, Z.-c. Wu and C. Zhou, Concentration quenching and thermal stability of Eu^{2+} emission in green emitting phosphor Li_2BaSiO_4: Eu^{2+}, *Solid State Sci.*, 2020, **99**, 106050.

2 G. Blasse., Luminescence of inorganic solids: From isolated centres to concentrated systems, *Prog. Solid St. Chem.*, 1988, **18**, 79-171.

3 D. L. Dexter, A Theory of Sensitized Luminescence in Solids, *J. Chem. Phys.*, 1953, **21**, 836-850.

4 R. Zhou, C. Liu, L.Lin, Y. Huang and H. Liang, *Chem. eng. J.*, 2019, **369**, 376-385.

5 R. Zhou, F. Ma, F. Su, Y. Ou,Z. Qi, J. Zahng, Y. Huang, P. Dorenbos and H. Liang, *Inorg. Chem.*, 2020, **59**, 17421-17429.